THE JOURNAL OF PHYSICAL CHEMISTRY B

Article

pubs.acs.org/JPCB

Understanding the Solvent Polarity Effects on Surfactant-Capped Nanoparticles

Sukit Leekumjorn,[†,∥] Sravani Gullapalli,[†,∥] and Michael S. Wong*[,†,‡,§]

[†]Department of Chemical and Biomolecular Engineering, [‡]Department of Chemistry, and [§]Department of Civil and Environmental Engineering, Rice University, 6100 Main Street, MS-362, Houston, Texas 77251-1892, United States

ABSTRACT: Understanding the molecular interactions between suspended nanoparticles (NPs) and the suspending solvent fluid may provide a useful avenue to create and to study exotic NP ensembles. This study focused on using a coarse-grained computational model to investigate the molecular interactions between oleate-capped NPs in various solvents, and to relate the results to experimental features of solvent-suspended, oleate-capped CdSe quantum dots (QDs). The QDs were modeled as a closed-shell fullerene molecule with an oleate-like ligand attached to each vertex. Solvent polarity was found to correlate to the simulation and experimental results more strongly than either dielectric constant or dipole moment. Computational results showed that the nonpolar solvents of hexane, toluene, and benzene (polarity index $E_T^N < 0.120$) kept NPs in suspension and solvated the oleate chains such that the oleate layer swelled to full extension. In contrast, as the most polar solvent tested ($E_T^N = 1.000$), water caused NPs to aggregate and precipitate. It partially solvated the oleate chains and compressed the layer to 86% of full extension. For solvents of intermediate polarity like ethanol, acetone, and chloroform, the oleate layer swelled with decreasing polarity index values, with rapid swelling occurring close to $E_T^N = 0.307$ (~50:50 vol % chloroform/acetone) below which QDs were colloidally stable. This study represents the first attempt to delineate the solvent effect on surfactant-coated NP hydrodynamic size, colloidal stability, and aggregation behavior.

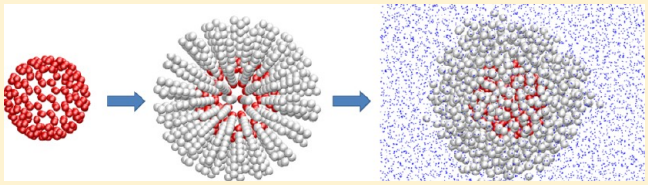

INTRODUCTION

Surfactant-capped nanoparticles (NPs) can nowadays be prepared through high-temperature slow-decomposition, hot-injection, and hydrothermal methods with great precision in chemical composition, size, and shape.[1−11] Typified by metal chalcogenide quantum dots (QDs), such NPs are generally synthesized in high-boiling-point organic liquids and processed using a variety of antisolvents and solvents. During the purification stage of NP synthesis, different liquids or liquid mixtures are used alternately to "crash out" and resuspend NPs to remove excess or unreacted species. Little attention is paid, though, to the interaction of the suspending fluid (hereafter referred to as a solvent) with the NPs and their surfactant layers, and how this relates to their colloidal stability. It is worthwhile to investigate the subtle differences of solvents on NP aggregation from a molecular perspective.

Information with regard to solvent effects on colloidal behavior of surfactant-capped NPs is scattered. Mattoussi et al. investigated the interparticle interactions of CdSe QDs and their dependency on the capping shell, surface coverage, particle size, and solvents through small-angle X-ray scattering.[12] They concluded that the most stable QDs were those covered with long-chain capping ligands, in which interactions between the ligand and solvent dominate over NP core−core interactions. They also concluded that low-to-moderate screening of core−core interactions can be achieved by increasing surface coverage of short-chain capping ligands to enhance ligand−solvent interactions.

In a different study, Fani et al. investigated the effects of capping ligand and solvents on CdS QD phase-transfer from organic solvent to water.[13] The highest phase-transfer efficiency was found for the hexane−oleic acid combination, compared to the chloroform−octylamine combination. There was evidence of partial NP aggregation with the hexane−oleic acid combination, which likely helped increase NP phase transfer efficiency. Yu et al. studied the effect of different ligands (oleic acid, elaidic acid, and stearic acid) on the chemical stability of CdTe QDs.[14] They found that oleic acid gave more stable NPs, which they attributed to the less crystalline packing of the hydrocarbon tail within the ligand surface layer. Furthermore, Saunders et al. utilized solvent−ligand interactions to controllably grow uniformly sized NPs and packed them into macroporous nanocrystal films.[15] Here using water droplets as a temporary template, NPs coated with appropriate ligands are packed into very ordered arrays. These studies indicate that the driving force for NP aggregation is associated more with solvent−ligand interactions than with core−core interactions.

Computational studies have been shown to provide much insight into solvent−ligand interactions, but there have been very few investigating the aggregation of ligand-capped NPs at a molecular level.[16] Among these studies, Glotzer and co-workers were among the first to investigate the formation of NP assemblies using implicit solvent Monte Carlo (MC) and

Received: August 10, 2012
Revised: October 5, 2012
Published: October 22, 2012

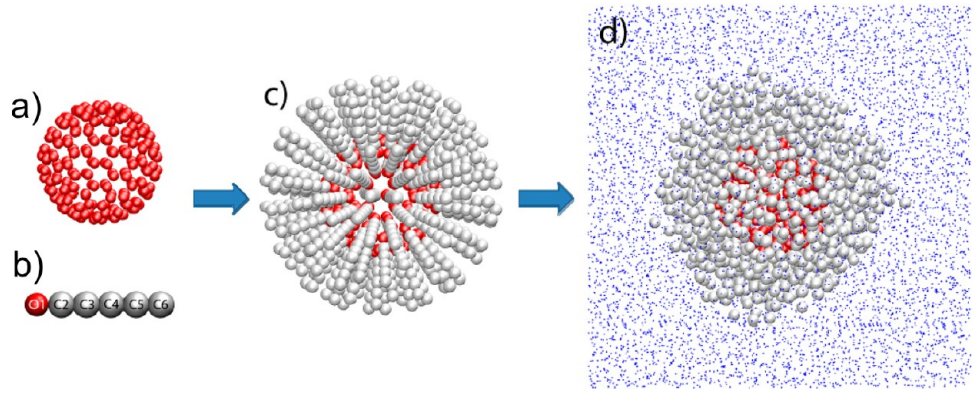

Figure 1. Course-grained model structures used for (a) the NP core, adapted from fullerene C_{180}, and (b) one oleate molecule in the MARTINI force-field. Colors correspond to the oleate headgroup (red) and hydrocarbon tail (gray). (c) Initial structure of the oleate-capped NP model and (d) a snapshot of the NP equilibrated in a solvent.

Brownian dynamics (BD) simulations.[17−19] For example, they studied the nanostructure networks formed by polyhedral oligomeric silsesquioxane (POSS), modeled by a coarse-grained NP consisting of one large cube as the inorganic core and a series of smaller cubes as the organic protective chains attached to the inorganic core.[17] By varying the organic chain length in the modeled molecules, they systematically studied the packing properties of the nanostructure, including the porosity, spatial distribution of NP building blocks, and extent of cross-linking, which were comparable to laboratory measurements of POSS aggregates. This work was further carried out by Chan et al.,[20] investigating the aggregation of polymer-tethered POSS in hexane using a new coarse-grained (CG) model (implicit solvent) in comparison to the all-atoms model (explicit solvent). Their findings suggested comparable results between the two models, where POSS molecules exhibit a localized packing feature of the silsesquioxane cages and tether conformations. By using the new CG model, they reduced simulation time by a factor of 100−10000, affording a savings in computing time of roughly 2 orders of magnitude.

Pileni and co-workers carried out both experimental and theoretical studies to predict and investigate the influence of the NP sizes (4−7 nm) in nonpolar solvents (cumene, hexane, octane, and toluene) on the growth of two-dimensional ordered sheets of 1-dodecanethiol-capped gold NPs via solvent evaporation.[21] Their MC and BD simulation results correlated well with experiment, indicating that structure formation was primary controlled by solvent-mediated interactions and not van der Waals attraction between NP cores. This was confirmed by the all-atom simulation study of C_{60} fullerenes by Girifalco[22] and the coarse-grained simulation studies of In't Veld et al.[23] and Lee and Hua,[24] in which they found the effective interaction range between NPs to be short regardless of the particle size. Thus, the presence of a protective layer can substantially reduce the van der Waals interactions between two NPs.[24]

Recently, Kaushik and Clancy reported the modeling of surfactant-coated NPs using an all-atom model in vacuum.[25] Two lead selenide (PbSe) NPs with a core size of 3−6 nm, attached by alkyl chain ligands (8−18 Å, 1.5−4 ligands/nm^3) were selected for simulations. They investigated the chain conformations for a single NP and pairs of NPs with respect to the core size, ligand length, and grafting density. Comparing the results with those from two united-atom models for the alkyl chains, they concluded that the choice of model can lead to an unrealistic NP behavior.

Modeling the solvent environment explicitly instead of implicitly can provide additional insights, though not many such computational studies on the structural and dynamics properties of ligand-capped NPs have appeared in the literature. The challenges and difficulties associated with these studies are (1) the simulation setting to mimic the experimental conditions, (2) the simulation force-fields that correctly describe the properties of solvent, NP, and their interactions, and (3) the size of the simulation matrix. As demonstrated in a recent study, Dai and co-workers utilized all-atom molecular dynamics (MD) simulations to study the self-assembly of C_{60} fullerenes (uncapped) at the water−trichloroethene (TCE) interface.[26] In their simulations, each fullerene started to migrate toward the water−TCE interface and self-assembled into a cluster near the interface. By incorporating free sodium dodecyl sulfate (SDS) surfactants in the solvent, they observed distinctive clustering of C_{60}'s at different surfactant concentrations.[27] MD simulations provided a wealth of information regarding the NP assembly process: (1) interfacial properties were influenced by surfactants, (2) the appearance of surfactant ordering increased with increasing surfactant concentration but independent of NP concentration, and (3) the NP assembly occurred at the liquid−liquid interface with or without surfactant.

In a related study, Kumar and co-workers investigated the self-assembled structure of cobalt NPs (40^3 lattice size = 384 atoms) in toluene (3400 per NP) in the presence of free sodium bis(2-ethylhexyl) sulfosuccinate using the combination of density functional theory (DFT) calculations and MC simulations.[28] Their findings showed that the NPs quickly form small aggregates and then into larger uniform aggregates of 4.7 nm, corresponding well to experimental results. Striolo and Egorov investigated the effect of two polymer grafted spherical colloidal particles in an implicit (good) solvent and explicit polymeric solvent using DFT calculations and MC simulations.[29] Their findings showed repulsive interactions between particles in the implicit solvent regardless of grafting density or grafted chain length but somewhat attractive in polymer solution with chain length greater than the grafted chain. The explicit solvent model provides additional information on how the grafted chains interact with the solvent, which is lacking in the implicit solvent model.

In this study, we developed coarse-grained computational models to investigate the molecular interactions between oleate-capped NPs in solvents. We coarse-grained oleate-capped CdSe QDs as closed-shell fullerenes with an attached ligand layer, and evaluated the layer thickness and aggregation propensity in several explicitly modeled solvents. Comparing the simulation results with dynamic light scattering analysis of oleate-capped CdSe QDs, we found that the ligand layer can swell depending on the solvent type, correlating well with the solvents experimentally tested. This study represents the first attempt to obtain a comprehensive understanding of the solvent effect in surfactant-capped NP colloidal stability.

EXPERIMENTAL AND COMPUTATIONAL METHODS

Simulation Details. With limited computational power and resource for large scale simulations in explicit solvents, molecular modeling of suspended NPs that consist of an inorganic core and an organic capped layer is a challenging task. To address this issue, we adopted a coarse-grained model using the MARTINI force-field for this study.[30,31] Since this force-field is primarily optimized for organic molecules and does not account for inorganic molecular topologies, we treated a surfactant-capped NP as a hollow core that is surrounded by an organic layer. An imaginary carbon framework of a C_{180} fullerene was used and oleate molecules, coarse-grained of 6-bead chains, were placed around NP as the protective layer (180 oleates per one NP), with the terminal end of the oleate molecule pointing outward from the NP center (Figure 1a–c).

After the NP was constructed and selected solvents were inserted into the simulation box, MD simulations were carried out to equilibrate the system (Figure 1d). The oleate packing density was controlled by the spacing of the fullerene framework, which was set at 0.35 nm from center to center between two adjacent carbon atoms, resulting in a core diameter of ~3.0 nm. This model approximates oleate-capped CdSe QDs with an inorganic diameter of 3.0 nm CdSe NPs carrying ~160 oleate ligands, based on the ~42 wt % organic content determined through thermogravimetric analysis.[32] Solvent molecules cannot penetrate the C_{180} hollow framework, which mimics the hardness of the inorganic core. Since this model of the capped NPs does not have information about the inorganic content, only short-range molecular interactions between the solvent molecules and oleate ligands are considered in our simulations. On the basis of recent findings by Pileni and co-workers that NP core–core interactions are less dominant in solution during the assembly process,[21] we believe that our model is applicable for NP studies in different solvents.

The seven solvents selected for this study were acetone, benzene, chloroform, ethanol, hexane, toluene, and water. Although a large selection of solvents is optimized in the MARTINI force-field (version 2.0), hexane and toluene molecules were unavailable. As respective substitutes for hexane and toluene, the octane force-field (consisting of two coarse-grained beads) and modification of the benzene force-field (adjusting the Lennard-Jones potential parameters on one of the three coarse-grained beads to compensate for the additional methyl group) were used. Since the coarse-grained octane was used in place of hexane during the simulations, we expected a slight adjustment in the molecular volume of solvent which reflects the number of solvent molecules within a simulation box. Furthermore, it has been shown that freezing of coarse-grained water molecules is a major issue in the MARTINI force-field (version 2.0) at 290 ± 5 K, and the presence of a solid interface can potentially enhance the freezing feature.[30,33] On the basis of the simulations considered in this study at 300 K, we did not find evidence of water freezing, as the NPs freely moved in the fluid.

Two sets of simulations were considered in this study, single and multiple NP systems. Single NP simulations were carried out for 200 ns to investigate the interactions between oleate chains and solvents without the influence of neighboring NPs. For this study, changes in the structural properties of the oleate layer were identified from the simulation trajectories. The systems were then enlarged by duplicating the simulation box three times in the *x*-, *y*-, and *z*-directions amounting to a total of 27 NPs. These larger systems were aimed at investigating the dynamic behavior of NPs concentrated in the selected solvent, with a total simulation time of 200 ns. System compositions are summarized in Table 1.

Table 1. Composition of Oleate-Capped NPs in Different Solvents, Listed Alphabetically[a]

solvent	# surfactant/NP	# solvent/NP
acetone	180	6728
benzene	180	4248
chloroform	180	6728
ethanol	180	6728
hexane	180	3329
toluene	180	4248
water	180	6728

[a]Two set of simulations consisting of 1 and 27 NPs were considered in this study. Note that the number of solvents per NP varies significantly to maintain the same volume of the simulation box.

All simulations were performed in the isothermal–isobaric (NPT) ensemble. The temperature and pressure of the simulation box were kept constant using the weak coupling technique,[34] with correlation times τ_T = 0.1 ps and τ_P = 0.5 ps for the temperature and pressure, respectively. The temperature for all systems was set at 300 K. Constant pressure was attained by adjustment of the three Cartesian directions (isotropic pressure coupling) to a pressure of P = 1 bar (compressibility k = 1×10^{-5} bar^{-1}). Periodic boundary conditions were imposed in all three directions. The simulation time-step was set at 4 fs using the leapfrog integration method.[35] Nonbonded interactions were cut off beyond 1.2 nm. Trajectories were collected every 20 ps. All simulations were performed with the GROMACS 4.0.5 software package[36–39] (single-precision mode) in parallel using the Shared University Grid at Rice-SUG@R cluster (2.83 GHz Intel Xeon E5440 quad core processors).

CdSe QD Synthesis and Characterization. Oleate-capped CdSe NPs were synthesized through the hot-injection route as previously reported.[3,5,40] The cadmium precursor was prepared by heating 0.128 g of CdO (99.99% Sigma Aldrich) in 2 mL of oleic acid (99.99% Sigma Aldrich) and 20 mL of octadecene (ODE, 90% Sigma Aldrich) under an argon atmosphere, until the mixture turned colorless. The selenium precursor was prepared by ultrasonicating 119 mg of Se metal (99.99% Sigma Aldrich) with 1 mL of trioctylphosphine (TOP, 90% Sigma Aldrich), until a clear solution was formed. The Se precursor (0.32 mL) was injected rapidly into a round-bottom flask containing an octadecene–cadmium oleate mixture at 250

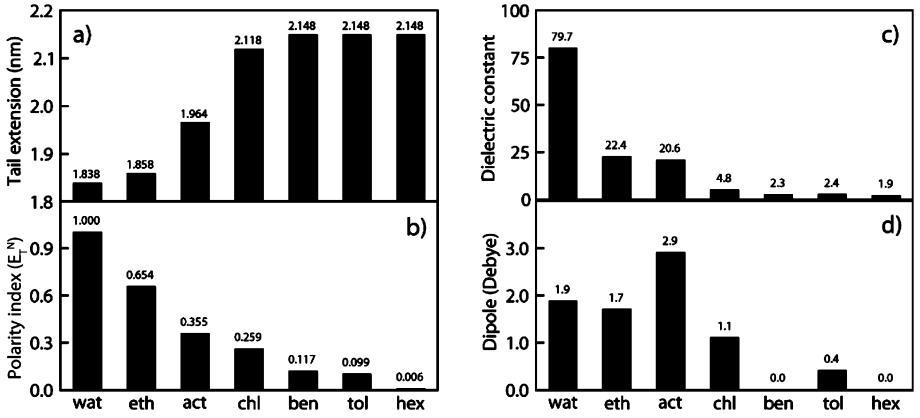

Figure 2. Correlation between solvent properties and oleate tail length in solvents. (a) Distance of the tail length estimated from the first RDF maximum peak between O1−C6 of oleate molecule for an oleate-capped NP in water ("wat"), ethanol ("eth"), acetone ("act"), chloroform ("chl"), benzene ("ben"), toluene ("tol"), and hexane ("hex"). Tabulated values for (b) solvent polarity index at 25 °C,[43] (c) dielectric constant at 20 °C,[44] and (d) dipole moment at 20 °C.[44]

°C under an argon blanket. The reaction flask temperature dropped to 220 °C and was kept at this temperature; 3 min after injection, the reaction flask was allowed to cool down to room temperature. The QDs were then washed several times using acetone and hexane. The QD stock suspension was prepared by drying the washed QDs and redispersing them in hexane.

To study the solvent effect on the QDs, hexane stock solution was divided equally into seven vials. The samples were then dried at room temperature under a vacuum overnight to remove the residual hexane. Dried samples were redispersed into various solvents: hexane (99.99% EMD, UN1208), toluene (99.5% EMD, UN1294), benzene (99.0% EMD, UN1114), chloroform (99.8% Sigma-Aldrich, 472476), acetone (99.7% Fisher, A18), ethanol (200 Proof Decan, 2701), or deionized (DI) water (18.2 MΩ-cm Barnstead Nanopure Diamond). The QD concentrations were ∼20 mg/mL in all samples, approximating the NP concentrations in the large simulation (27 NPs) systems.

Transmission Electron Microscopy (TEM) and Size Analysis. A drop of the dilute sample was placed onto a carbon coated TEM grid (PELCO ultrathin carbon film supported by a lacey carbon film on a 400 mesh copper grid) and dried. TEM measurements were performed on a JEOL 1230 high contrast transmission electron microscope (80 kV accelerating voltage). Digital micrograph software was used to record the images detected by the CCD camera, and Image J software was used for the particle size analysis.

Optical Measurements. In this work, a Shimadzu UV−visible spectrophotometer (UV-2401PC) was used to make all the absorbance measurements using a standard quartz cuvette with a light path length of 1 cm. The fluorescence measurements were done on the SPEX-Fluoromax-3 fluorimeter at an excitation wavelength of 480 nm.

The quantum yield (QY) measurements were carried out using the following protocol.[41] The absorbance and emission spectra of the standard as well as the test sample, at different concentrations, were measured. A linear plot of the integrated intensity versus absorbance at the excitation wavelength was obtained where the slope is proportional to the QY of the different samples. QY was then calculated using eq 1, where the subscript ST denotes the standard sample and the subscript X denotes the test sample. RI is the solvent refractive index.

$$\left(\frac{QY_X}{QY_{ST}}\right) = \frac{Slope_X}{Slope_{ST}} \frac{RI_X^2}{RI_{ST}^2} \quad (1)$$

Dynamic Light Scattering (DLS) Measurements. DLS experiments were performed on the Brookhaven ZetaPALS dynamic light scattering equipment with a BI-9000AT digital autocorrelator at a 90° scattering angle. All experiments were done at room temperature using undiluted QD suspensions and a 656 nm wavelength source. The number-intensity-based hydrodynamic diameters for QDs were calculated using the appropriate CONTIN or the NNLS routine. The ∼20 mg/mL concentrations were close to those in the large simulation box study.

RESULTS AND DISCUSSION

Computational Results for Simulation Box with 1 NP. Simulations of a single NP were carried out different solvents to determine the feasibility of the model and to identify interactions between surfactant and solvent molecules in the absence of neighboring NPs. On the basis of the simulation trajectories, it was observed that the perturbations of oleate molecules in solution were different depending on the solvent type. The average distance of oleate molecules stretching from the core outward was measured using the radial distribution analysis between the first and last beads (O1 and C6 beads, respectively) of the oleate chain. As shown in Figure 2a, the ensemble average oleate length increased from the water case (1.84 nm) to the chloroform case (2.12 nm), reaching the extension length of 2.15 nm for the benzene, toluene, and hexane cases.

The solvent properties of dielectric constants (ε) and dipole moments (μ), which are commonly used to describe the polarity of solvents, did not correlate well with calculated tail length (Figure 2c and d). On the other hand, normalized molar electronic transition energies (E_T^N) correlated well with calculated tail length (Figure 2b). These E_T^N values are derived from UV−vis absorption spectra of a solvatochromic pyridinium *N*-phenolate betaine dye solubilized in a particular solvent at 25 °C and 1 bar, referenced to the same dye dissolved in water (as the most polar solvent) and in tetramethylsilane (as the most nonpolar solvent). These values, tabulated for hundreds of solvents, range from 0 (for the least polar solvent) to 1 (for the most polar).[42]

dx.doi.org/10.1021/jp307985c | J. Phys. Chem. B 2012, 116, 13063−13070

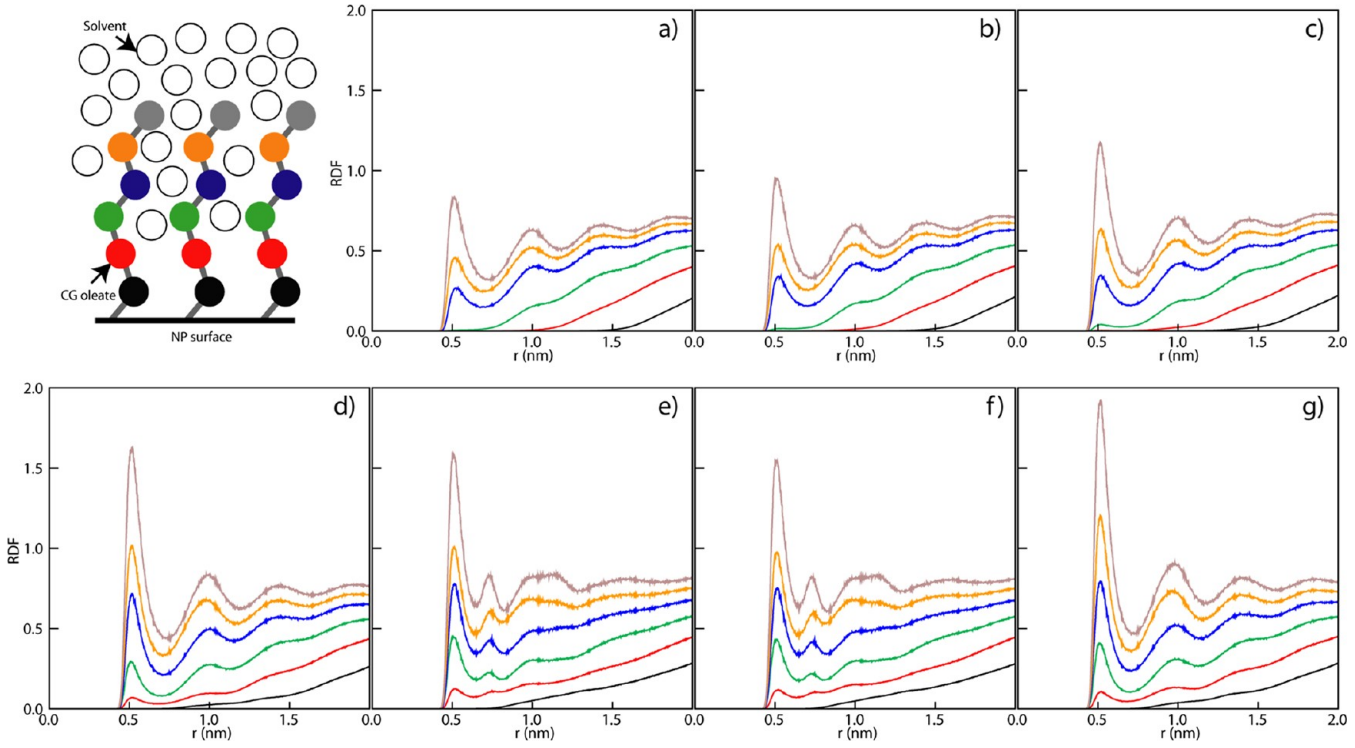

Figure 3. RDF between oleate and solvent molecules for (a) water, (b) ethanol, (c) acetone, (d) chloroform, (e) benzene, (f) toluene, and (g) hexane. The cartoon drawing corresponds to the correlation between O1 (black), C2, (red), C3 (green), C4 (blue), C5 (orange), and C6 (gray) of oleate and respective solvents.

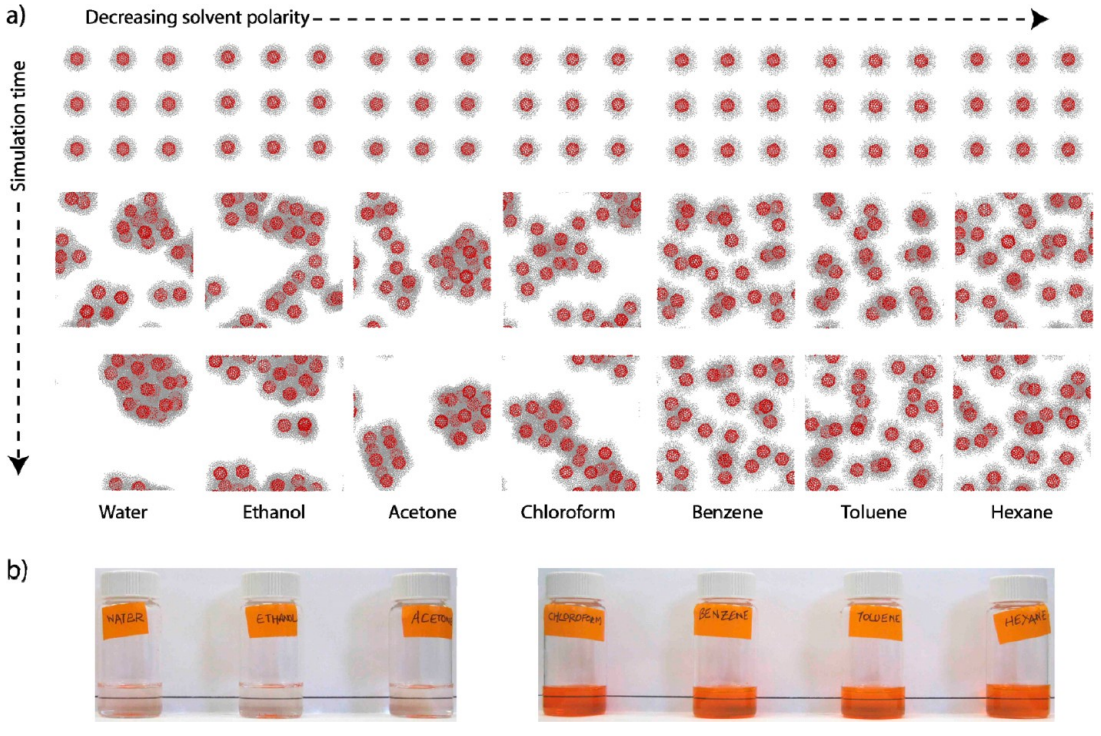

Figure 4. (a) Snapshots of simulation trajectory for the multiple NP simulations. Comparative ranking of NP in the selected solvent is shown from left to right with decreasing solvent polarity. Simulation progress is shown from top to bottom. For clarity, solvent molecules are not shown. (b) Corresponding CdSe QDs redisperse in different solvents.

The radial distribution functions (RDFs) showed a peak at ~0.512 nm for the C4, C5, and C6 positions of the coarse-grained oleate chain, indicating they were in contact with the solvent molecules (Figure 3a and b). The RDFs did not show this peak below the C4 position, indicating that the solvent molecules did not penetrate below C4 to contact the lower bead positions. This result is consistent with a compact oleate coating, which was quantified with a short tail extension (Figure

dx.doi.org/10.1021/jp307985c | J. Phys. Chem. B 2012, 116, 13063−13070

2a). In acetone, the RDFs showed that the solvent molecules reached the C3 position, consistent with a slightly more swollen oleate layer (Figure 3c). With solvents of decreasing polarity (as ranked by E_T^N values), the respective solvent molecules penetrated more deeply through the oleate layer, such that the O1 position was reached (Figure 3d–g).

On the basis of the RDF results, the swelling of the oleate was directly related to the penetration of the solvent molecules into the layer, and the extent of penetration into the oleate layer depended on solvent polarity. For the solvents of water, ethanol, acetone, chloroform, benzene, toluene, and hexane, the number of solvent molecules trapped within the swollen oleate layer per NP was estimated to be 200–600. These values were estimated by counting the number of solvent molecules only within the first correlation peak between oleates and solvents, which was set between 0 and 0.512 nm for the first solvation layer. The solvent molecules within the first solvation layer were assumed to be the predominant driving force for ligand–solvent interactions.

Computational Results for Simulation Box with 27 NPs. To consider NP aggregation behavior in different solvents through dynamic simulations, we constructed model systems of several NPs by enlarging the single NP simulations with the respective solvents. Figure 4a (top row) shows the initial snapshot of the simulation box with 27 NPs. The system settings were such that there were no interactions between NPs initially and the driving force was associated with the interactions between oleate and solvents. The NPs were not in equilibrium initially, and selected snapshots of the simulation trajectory (Figure 4a, second and third rows) were used to identify the dynamic movement of NPs.

In hexane, toluene, and benzene, NP movement was found to be random and NPs did not aggregate with one another, mimicking Brownian motion of dispersed particles. In water and ethanol, on the other hand, NPs quickly formed aggregates with one another. In acetone, NPs aggregated also, though the oleate layer was slightly more solvated compared to the cases of water and ethanol, as indicated by the 1-NP simulations (Figure 2a). In chloroform, the NPs aggregated, even though the oleate layer was swelled nearly as much as the hexane, toluene, or benzene cases (Figure 2a). Any aggregation of NPs was due to hydrophobic interactions between the oleate layers of NPs, as simulated by the short-range Lennard-Jones interactions of the MARTINI force-field.

Oleate-capped CdSe QDs could not be dispersed in water, ethanol, and acetone, and could be dispersed in chloroform, benzene, toluene, and hexane (Figure 4b). These experimental observations were consistent with simulation results for all solvent cases, except for chloroform. The observed lack of QD precipitation using chloroform as the solvent suggested that QDs formed small aggregates that remained in suspension.

The extent of NP solvation was assessed as a function of simulation time for each solvent case. The number of solvent molecules surrounding the oleate layer for each of the 27 NPs was estimated within the first correlation peak between oleates and solvents, which was set between 0 and 0.512 nm (Figure 3). The total number of solvent molecules was determined, up to a simulation time of 200 ns, for each solvent (Figure 5). The number of solvent molecules remained the same for the toluene, benzene, and hexane, correlating to the fully solvated, unaggregated state of the oleate-capped NPs.

There was a significantly larger amount of benzene and toluene molecules around the NPs than compared to the hexane case, because benzene and toluene molecules occupy a smaller volume per molecule than hexane, and therefore more can fit within a given volume (cf. molar volumes of benzene, toluene, and hexane at 25 °C are 89.4,[45] 107.0,[46] and 147.5 cm^3/mol,[47] respectively). Simulations indicated comparable benzene and toluene numbers, even though benzene had a smaller molar volume, suggesting that the stronger dipole moment of toluene allowed for greater solvation of the polar headgroup of the oleate molecule at the NP surface.

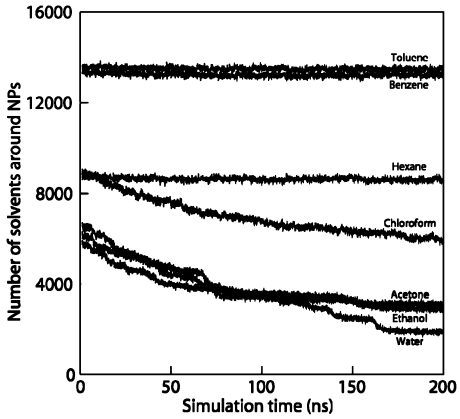

Figure 5. Ensemble average number of solvent molecules within the oleate layer for 27 NPs as a function of simulation time. Averages were estimated within the first hydration layer of the oleate molecule.

For water, ethanol, and acetone, the total number of solvent molecules decreased with time, which can be associated with deswelling of the oleate layer. The observed stepwise decrease was due to aggregation of the NPs, expelling additional solvent molecules from the oleate layer. For chloroform, the total number of solvent molecules decreased. Since the 1-NP simulation results indicated the oleate layer remained essentially swollen, this decrease could be due to a type of NP aggregation process in which expulsion of solvent molecules did not occur stepwise.

Characterization of CdSe QDs Dispersed in Different Solvents. QDs suspended in chloroform, benzene, toluene, and hexane were analyzed via TEM (Figure 6). The average particle core diameters based on ~200 particles for each solvent case were 3.72, 3.60, 3.49, and 3.27 nm, respectively, all within one standard deviation of each other (Table 2). No TEM evidence of small QD aggregates was observed for the chloroform case, as suggested earlier by the simulation results.

The hydrodynamic diameters measured via DLS were roughly the same for the hexane, toluene, and benzene cases, while the chloroform case yielded a smaller hydrodynamic diameter. The average oleate layer thickness was estimated as half the difference between the hydrodynamic diameter and the core size (Table 2). These experimental values were qualitatively consistent with the CGMD simulation results for the oleate tail thickness (Figure 2a).

To determine whether the QDs were fully dispersed or partially aggregated in solutions as observed from the simulations, quantum yield (QY) measurement was used. A decrease in the quantum yield may be associated with the quenching effects due to partial aggregation of QDs in a given solvent.[49–51] We note that other phenomena such as chemical degradation and interaction of oxygen or water with the QD surface that result in localized surface defects (and can lead to a decrease in QY) cannot be ignored.[52–55] From Table 2, the

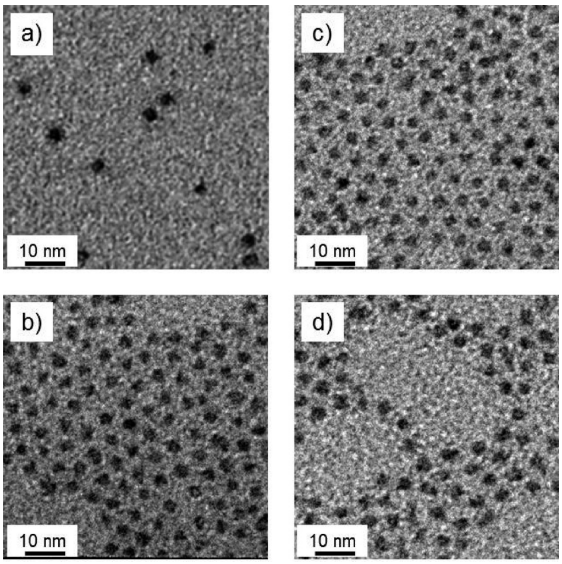

Figure 6. TEM images of the oleate-capped CdSe QDs in (a) hexane, (b) toluene, (c) benzene, and (d) chloroform.

QYs increased in the order of chloroform, benzene, toluene, and hexane. We speculate that the highly solvated oleate layer provides access to the QD surface, and the more electronically active solvents (e.g., with higher dipole moments and higher dielectric constants) interfere with the radiative recombination pathway, thus lowering the QY.

The Chloroform Case. The computational and experimental data can be summarized in Figure 7, in which NPs precipitate in the blue region (which includes the polar solvents of water, ethanol, and acetone), and do not precipitate in the red region (which includes the nonpolar solvents of chloroform, benzene, toluene, and hexane). These regions correlate to the computationally calculated oleate tail length, with length variations due to swelling by solvent molecules. There is a transition point between acetone (E_T^N = 0.355) and chloroform (E_T^N = 0.259) at which macroscopic precipitation (i.e., suspension cloudiness) occurs. We conducted NP precipitation experiments using chloroform/acetone mixtures and found that a mixture containing chloroform at a volume percent of 49.9–50.1% induces NP aggregation. This mixture has an effective solvent polarity index of 0.307, using the Snyder formula.[56]

Whereas water, ethanol, and acetone were predicted through multi-NP simulations to induce NP aggregation (which matched the experimental observations), chloroform was also predicted to induce NP aggregation even though it is a "good" solvent for QDs (Figure 4). The possibility of the NPs forming small aggregates that remained in suspension was not supported by DLS results. Single-NP simulations indicated the oleate layer remained nearly fully swollen, yet multi-NP simulations indicated solvent expulsion from the oleate layer.

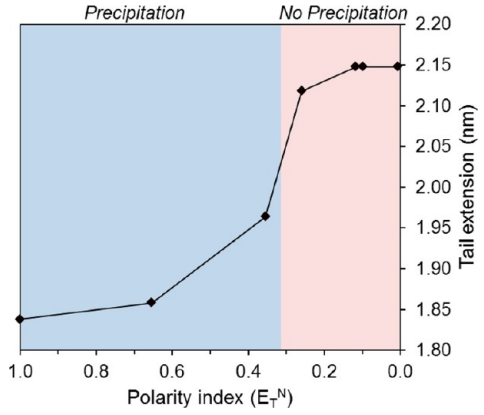

Figure 7. Computed oleate extension and observed precipitation behavior of oleate-capped QDs in suspending fluids of varying solvent polarity and computed oleate length.

We suggest that oleate-capped QDs exhibit rapid and reversible aggregation in which the oleate ligands on one particle interdigitate with those of another.

CONCLUSION

In this study, experimental work with CdSe QDs and computational work with a model NP structure were performed to gain insight into how solvent polarity played a role in surfactant-capped NP colloidal stability. Molecular dynamics simulations of single oleate-capped NPs showed the oleate layer swelled to different extents depending on the solvent type. Oleate lengths roughly matched experimental measurements of oleate thickness, with the layer being fully swelled and thickest in nonpolar solvents and the least swelled in water. Simulations of multiple NPs showed aggregation behavior that matched well with experimental observations for all solvents except chloroform; e.g., NPs were fully dispersed in hexane, toluene, and benzene. The polarity indices of chloroform and acetone are close in value, but the QDs were stable in the former and not the latter. The QD colloidal stability transition point was found with a chloroform–acetone mixture of ~50 vol %. Highlighting polarity as the key solvent feature for colloidal stability of surfactant-capped NPs, this computational approach should be useful for analyzing colloidal particles with more complex structures and other solvent types.

AUTHOR INFORMATION

Corresponding Author

*E-mail: mswong@rice.edu.

Author Contributions

‖These authors contributed equally to this work.

Notes

The authors declare no competing financial interest.

Table 2. Estimated QD Core Size, Hydrodynamic Diameter, Oleate Tail Extension, and Quantum Yield

solvent	core diameter from TEM (nm)	hydrodynamic diameter from DLS (nm)	oleate length[a] (nm)	RIs[b]	actual QY (%)	normalized QY[c]
chloroform	3.72 ± 0.53	7.41 ± 0.69	1.85 ± 0.61	1.446	7.6	0.61
benzene	3.60 ± 0.45	8.54 ± 0.80	2.47 ± 0.63	1.501	9.1 ± 0.45	0.73 ± 0.04
toluene	3.49 ± 0.46	8.57 ± 0.84	2.54 ± 0.65	1.497	11.8 ± 0.90	0.95 ± 0.07
hexane	3.27 ± 0.52	8.89 ± 0.90	2.81 ± 0.71	1.375	12.4 ± 0.60	1.00 ± 0.05

[a]Calculated as $^1/_2$ of the difference of hydrodynamic and core diameters. [b]Refractive indices (RIs) are from ref 48. [c]QY values normalized to the hexane case.

■ ACKNOWLEDGMENTS

The authors are grateful for partial financial support from 3M and Advanced Aromatics. The authors thank the Shell Center for Sustainability at Rice University (graduate fellowship to S.G.). Access to the computational resources was provided by the Shared University Grid at Rice-SUG@R. The authors also thank Dr. H. G. Bagaria and Dr. G. C. Kini for their comments and valuable discussion on the synthesis and characterization of CdSe QDs. Special thanks to Mr. C. Reuda (Institute of Biosciences and Bioengineering (IBB)-Howard Hughes Medical Institute (HHMI) Summer Program) for his efforts in creating the capped NP model.

■ REFERENCES

(1) Jun, Y. W.; Lee, S. M.; Kang, N. J.; Cheon, J. *J. Am. Chem. Soc.* **2001**, *123*, 5150−5151.
(2) Manna, L.; Milliron, D. J.; Meisel, A.; Scher, E. C.; Alivisatos, A. P. *Nat. Mater.* **2003**, *2*, 382−385.
(3) Asokan, S.; Krueger, K. M.; Colvin, V. L.; Wong, M. S. *Small* **2007**, *3*, 1164−1169.
(4) Cho, J. W.; Kim, H. S.; Kim, Y. J.; Jang, S. Y.; Park, J.; Kim, J. G.; Kim, Y. J.; Cha, E. H. *Chem. Mater.* **2008**, *20*, 5600−5609.
(5) Asokan, S.; Krueger, K. M.; Alkhawaldeh, A.; Carreon, A. R.; Mu, Z. Z.; Colvin, V. L.; Mantzaris, N. V.; Wong, M. S. *Nanotechnology* **2005**, *16*, 2000−2011.
(6) Murray, C. B.; Norris, D. J.; Bawendi, M. G. *J. Am. Chem. Soc.* **1993**, *115*, 8706−8715.
(7) Peng, X. G.; Manna, L.; Yang, W. D.; Wickham, J.; Scher, E.; Kadavanich, A.; Alivisatos, A. P. *Nature* **2000**, *404*, 59−61.
(8) Zhang, H.; Wang, L. P.; Xiong, H. M.; Hu, L. H.; Yang, B.; Li, W. *Adv. Mater. (Weinheim, Ger.)* **2003**, *15*, 1712−1715.
(9) Jun, Y. W.; Choi, J. S.; Cheon, J. *Angew. Chem., Int. Ed.* **2006**, *45*, 3414−3439.
(10) Fiore, A.; Mastria, R.; Lupo, M. G.; Lanzani, G.; Giannini, C.; Carlino, E.; Morello, G.; De Giorgi, M.; Li, Y.; Cingolani, R.; Manna, L. *J. Am. Chem. Soc.* **2009**, *131*, 2274−2282.
(11) Manna, L.; Scher, E. C.; Alivisatos, A. P. *J. Am. Chem. Soc.* **2000**, *122*, 12700−12706.
(12) Mattoussi, H.; Cumming, A. W.; Murray, C. B.; Bawendi, M. G.; Ober, R. *Phys. Rev. B* **1998**, *58*, 7850−7863.
(13) Fini, P.; Depalo, N.; Comparelli, R.; Curri, M. L.; Striccoli, M.; Castagnolo, M.; Agostiano, A. *J. Therm. Anal. Calorim.* **2008**, *92*, 271−277.
(14) Yu, W. W.; Wang, Y. A.; Peng, X. G. *Chem. Mater.* **2003**, *15*, 4300−4308.
(15) Saunders, A. E.; Korgel, B. A. *ChemPhysChem* **2005**, *6*, 61−65.
(16) Leekumjorn, S.; Wong, M. S. 5.07 - Self-Assembly of Nanoparticle Building Blocks. In *Comprehensive Nanoscience and Technology*; Academic Press: Amsterdam, The Netherlands, 2010; Vol. 5, pp 203−224.
(17) Lamm, M. H.; Chen, T.; Glotzer, S. C. *Nano Lett.* **2003**, *3*, 989−994.
(18) Zhang, Z. L.; Horsch, M. A.; Lamm, M. H.; Glotzer, S. C. *Nano Lett.* **2003**, *3*, 1341−1346.
(19) Zhang, Z. L.; Keys, A. S.; Chen, T.; Glotzer, S. C. *Langmuir* **2005**, *21*, 11547−11551.
(20) Chan, E. R.; Striolo, A.; McCabe, C.; Cummings, P. T.; Glotzer, S. C. *J. Chem. Phys.* **2007**, *127*, 1141021−11410215.
(21) Goubet, N.; Richardi, J.; Albouy, P. A.; Pileni, M. P. *J. Phys. Chem. Lett.* **2011**, *2*, 417−422.
(22) Girifalco, L. A. *J. Phys. Chem.* **1992**, *96*, 858−861.
(23) Veld, P. J. i. t.; Horsch, M. A.; Lechman, J. B.; Grest, G. S. *J. Chem. Phys.* **2008**, *129*, 164504−164507.
(24) Lee, C. K.; Hua, C. C. *J. Chem. Phys.* **2010**, *132*, 2249041−2249049.
(25) Kaushik, A. P.; Clancy, P. *J. Chem. Phys.* **2012**, *136*, 1147021−11470212.
(26) Luo, M. X.; Mazyar, O. A.; Zhu, Q.; Vaughn, M. W.; Hase, W. L.; Dai, L. L. *Langmuir* **2006**, *22*, 6385−6390.
(27) Luo, M.; Dai, L. L. *J. Phys.: Condens. Matter* **2007**, *19*, 3751091−3751014.
(28) Adhikari, N. P.; Peng, X. H.; Alizadeh, A.; Ganti, S.; Nayak, S. K.; Kumar, S. K. *Phys. Rev. Lett.* **2004**, *93*, 1883011−1883014.
(29) Striolo, A.; Egorov, S. A. *J. Chem. Phys.* **2007**, *126*, 0149021−0149025.
(30) Marrink, S. J.; Risselada, H. J.; Yefimov, S.; Tieleman, D. P.; de Vries, A. H. *J. Phys. Chem. B* **2007**, *111*, 7812−7824.
(31) Murtola, T.; Bunker, A.; Vattulainen, I.; Deserno, M.; Karttunen, M. *Phys. Chem. Chem. Phys.* **2009**, *11*, 1869−1892.
(32) Asokan, S. Chemical processing of colloidal cadmium selenide nanoparticles: New approaches to dimensional and morphological control, Rice University, 2008.
(33) Marrink, S. J.; de Vries, A. H.; Mark, A. E. *J. Phys. Chem. B* **2004**, *108*, 750−760.
(34) Berendsen, H. J. C.; Postma, J. P. M.; Vangunsteren, W. F.; Dinola, A.; Haak, J. R. *J. Chem. Phys.* **1984**, *81*, 3684−3690.
(35) Allen, M. P.; Tildesley, D. J. *Computer simulation of liquids*; Clarendon Press: Oxford, U.K., 1987.
(36) Hess, B.; Kutzner, C.; van der Spoel, D.; Lindahl, E. *J. Chem. Theory Comput.* **2008**, *4*, 435−447.
(37) Van der Spoel, D.; Lindahl, E.; Hess, B.; Groenhof, G.; Mark, A. E.; Berendsen, H. J. C. *J. Comput. Chem.* **2005**, *26*, 1701−1718.
(38) Lindahl, E.; Hess, B.; van der Spoel, D. *J. Mol. Model.* **2001**, *7*, 306−317.
(39) Berendsen, H. J. C.; Vanderspoel, D.; Vandrunen, R. *Comput. Phys. Commun.* **1995**, *91*, 43−56.
(40) Ko, W. Y. L.; Bagaria, H. G.; Asokan, S.; Lin, K. J.; Wong, M. S. *J. Mater. Chem.* **2010**, *20*, 2474−2478.
(41) Hariba, J. Y. *A Guide to Recording Fluorescence Quantum Yield*; Jobin Yvon Hariba Limited: Stanmore, U.K., 2003.
(42) Reichardt, C. *Chem. Rev.* **1994**, *94*, 2319−2358.
(43) Reichardt, C. *Angew. Chem., Int. Ed.* **1979**, *18*, 98−110.
(44) Smallwood, I. *Handbook of organic solvent properties*; Arnold: London, 1996.
(45) Leger, J. M. *Solid State Commun.* **1988**, *66*, 245−247.
(46) Franck, E. U.; Kerschbaum, S.; Wiegand, G. *Ber. Bunsen-Ges. Phys. Chem.* **1998**, *102*, 1794−1797.
(47) Funazukuri, T.; Nishimoton; Wakao, N. *J. Chem. Eng. Data* **1994**, *39*, 911−915.
(48) Šedivec, V.; Flek, J. *Handbook of analysis of organic solvents*; Halsted Press: New York, 1976.
(49) Kim, T.; Noh, M.; Lee, H.; Joo, S.-W.; Lee, S. Y.; Lee, K. *J. Phys. Chem. B* **2009**, *113*, 14487−14490.
(50) Liu, J.; Yang, X.; Wang, K.; Yang, R.; Ji, H.; Yang, L.; Wu, C. *Chem. Commun. (Cambridge, U.K.)* **2011**, *47*, 935−937.
(51) Resch-Genger, U.; Grabolle, M.; Cavaliere-Jaricot, S.; Nitschke, R.; Nann, T. *Nat. Methods* **2008**, *5*, 763−775.
(52) Katari, J. E. B.; Colvin, V. L.; Alivisatos, A. P. *J. Phys. Chem.* **1994**, *98*, 4109−4117.
(53) Mancini, M. C.; Kairdolf, B. A.; Smith, A. M.; Nie, S. *J. Am. Chem. Soc.* **2008**, *130*, 10836−10837.
(54) Noh, M.; Kim, T.; Lee, H.; Kim, C.-K.; Joo, S.-W.; Lee, K. *Colloids Surf., A* **2010**, *359*, 39−44.
(55) Yan, Y.; Wang, S.; Liu, Z.; Wang, H.; Huang, D. *Anal. Chem.* **2010**, *82*, 9775−9781.
(56) Issaq, H. J. *A century of separation science*; Marcel Dekker: New York, 2002.